British Journal of Pharmacology

DOI:10.1111/j.1476-5381.2010.01186.x
www.brjpharmacol.org

RESEARCH PAPER

Fenamates as TRP channel blockers: mefenamic acid selectively blocks TRPM3

Chihab Klose[1,2,3]*, Isabelle Straub[2,4]*, Marc Riehle[1], Felicia Ranta[5], Dietmar Krautwurst[6], Susanne Ullrich[5], Wolfgang Meyerhof[7] and Christian Harteneck[1,2]

[1]*Department of Pharmacology and Experimental Therapy, Institute of Experimental and Clinical Pharmacology and Toxicology, Interfaculty Center of Pharmacogenomics and Pharmaceutical Research (ICePhA), Eberhard-Karls-University, Tübingen, Germany,* [2]*Molecular Pharmacology and Cell Biology, Charité, Berlin, Germany,* [3]*Fachbereich Biologie, Chemie, Pharmazie, Freie Universität Berlin, Berlin, Germany,* [4]*Rudolf-Boehm-Institut für Pharmakologie und Toxikologie, Leipzig, Germany,* [5]*Department of Internal Medicine, Division of Endocrinology, Diabetology, Vascular Medicine, Nephrology, and Clinical Chemistry, Eberhard-Karls-University, Tübingen, Germany,* [6]*Deutsche Forschungsanstalt für Lebensmittelchemie, Molekulare Zellphysiologie und Chemorezeption, Freising, Germany, and* [7]*Abteilung Molekulare Genetik, Deutsches Institut für Ernährungsforschung Potsdam-Rehbrücke, Nuthetal, Germany*

Correspondence
Dr Christian Harteneck, Institute of Pharmacology and Toxicology, Eberhard-Karls-Universität, Wilhelmstr. 56, 72074 Tübingen, Germany. E-mail: christian.harteneck@uni-tuebingen.de

*The first two authors contributed equally to the work.

Keywords
cationic channel; transient receptor potential; non-steroidal anti-inflammatory drugs; fenamate; pancreatic β-cells

Received
17 June 2010
Revised
21 November 2010
Accepted
26 November 2010

BACKGROUND AND PURPOSE

Fenamates are N-phenyl-substituted anthranilic acid derivatives clinically used as non-steroid anti-inflammatory drugs in pain treatment. Reports describing fenamates as tools to interfere with cellular volume regulation attracted our attention based on our interest in the role of the volume-modulated transient receptor potential (TRP) channels TRPM3 and TRPV4.

EXPERIMENTAL APPROACH

Firstly, we measured the blocking potencies and selectivities of fenamates on TRPM3 and TRPV4 as well as TRPC6 and TRPM2 by Ca^{2+} imaging in the heterologous HEK293 cell system. Secondly, we further investigated the effects of mefenamic acid on cytosolic Ca^{2+} and on the membrane voltage in single HEK293 cells that exogenously express TRPM3. Thirdly, in insulin-secreting INS-1E cells, which endogenously express TRPM3, we validated the effect of mefenamic acid on cytosolic Ca^{2+} and insulin secretion.

KEY RESULTS

We identified and characterized mefenamic acid as a selective and potent TRPM3 blocker, whereas other fenamate structures non-selectively blocked TRPM3, TRPV4, TRPC6 and TRPM2.

CONCLUSIONS AND IMPLICATIONS

This study reveals that mefenamic acid selectively inhibits TRPM3-mediated calcium entry. This selectivity was further confirmed using insulin-secreting cells. K_{ATP} channel-dependent increases in cytosolic Ca^{2+} and insulin secretion were not blocked by mefenamic acid, but the selective stimulation of TRPM3-dependent Ca^{2+} entry and insulin secretion induced by pregnenolone sulphate were inhibited. However, the physiological regulator of TRPM3 in insulin-secreting cells remains to be elucidated, as well as the conditions under which the inhibition of TRPM3 can impair pancreatic β-cell function. Our results strongly suggest mefenamic acid is the most selective fenamate to interfere with TRPM3 function.

Abbreviations

DCDPC, 3′-5-dichlorodiphenylamine-2-carboxylic acid; HEK293 cells, human embryonic kidney cells; INS-1E cells, insulinoma beta-cells; NSAIDs, non-steroidal anti-inflammatory drugs; Mef, mefenamic acid; PregS, pregnenolone sulphate; TRP, transient receptor potential; TRPA, ankyrin-like TRPs; TRPM, melastatin-related TRPs; TRPML, mucolipidin-like TRPs; TRPP, polycystin-like TRPs; TRPV, vanilloid receptor-related TRPs

Introduction

Fenamates, N-substituted anthranilic acid derivatives, represent an important group of clinically used non-steroidal anti-inflammatory drugs (NSAIDs). The therapeutic use of mefenamic acid and others results from their inhibitory action on both cyclooxygenase enzymes and subsequent interference with the metabolites of the arachidonic pathway. By contrast, mefenamic acids such as tolfenamic acid, flufenamic acid, niflumic acid, meclofenamic acid and DCDPC (3′-5-dichlorodiphenylamine-2-carboxylic acid) have also been described to modulate a variety of ion channels and enzymes (Gögelein *et al.*, 1990; Kankaanranta and Moilanen, 1995; Vietri *et al.*, 2000; Guinamard *et al.*, 2004; Dvorzhak, 2008; Habjan and Vandenberg, 2009). The use of fenamates to interfere with cellular volume regulation (Jin *et al.*, 2003; Lambert and Oberwinkler, 2005; Ducharme *et al.*, 2007; Numata *et al.*, 2007) as well as reports describing flufenamic acid as a blocker of transient receptor potential (TRP) channels attracted our interest to this group of small compounds (Tesfai *et al.*, 2001; Lee *et al.*, 2003; Guinamard *et al.*, 2004; Hill *et al.*, 2004; Guilbert *et al.*, 2009). In fact, the use of flufenamic acid is increasing because of the absence of selective and potent drugs or pharmacological tools to interfere with TRP channel activity. Although flufenamic acid belongs to a large family of chemically related compounds (fenamates), their actions on TRP channels are largely unknown.

TRP proteins form a superfamily of non-selective cation channels comprising at least 27 members in mammals (Harteneck *et al.*, 2000; Montell *et al.*, 2002; Clapham *et al.*, 2005). Sequence identification and the cloning of the prototypic channel, *Drosophila* TRP, provided the template for the identification of TRP homologous genes in the worm, fly, fish and mammalian genomes by sequence comparison (Montell and Rubin, 1989). Based on sequence similarity and functional aspects, the mammalian TRP superfamily comprises six subfamilies: classic or canonical TRPs (TRPC), vanilloid receptor-related TRPs (TRPV), melastatin-related TRPs (TRPM), ankyrin-like TRPs (TRPA), polycystin-like TRPs (TRPP) and mucolipidin-like TRPs (TRPML). TRPC members are typically activated by G-protein-coupled receptors via phospholipase C (PLC) (Beech *et al.*, 2009). Increases in temperature activate four out of six TRPV channels, providing evidence for their involvement in heat and pain sensations in the human body (Talavera *et al.*, 2008). TRPV5 and TRPV6 channels have been characterized as ion channels with high selectivity for calcium in duodenal and renal epithelia (Vennekens *et al.*, 2008; Vriens *et al.*, 2009). The TRPM channels (eight members) possess a variable permeability for divalent cations and are activated by a spectrum of diverse stimuli, for example hydrogen peroxide, menthol, cold, icilin, calcium hypotonicity and sphingosine (Harteneck, 2005; Kraft and Harteneck, 2005). In mammals, the TRPA family consists of only one member TRPA1, which is involved in nociceptive and cold sensation (Caspani and Heppenstall, 2009). Polycystin TRPs (TRPP2, -P3 and -P5) form channels in the plasma membrane as well as intracellular membranes, and are probably integrated in complexes with the receptor-forming polycystin P1 and P4 proteins (Delmas, 2005). TRPML form lysosomal ion channels (Puertollano and Kiselyov, 2009).

Here, we examined the inhibitory effect of several available fenamates (DCDPC, flufenamic acid, mefenamic acid, meclofenamic acid, niflumic acid, S645648, tolfenamic acid) on the TRPM3 and TRPV4 channels using fluorescence-based FLIPR Ca^{2+} measurements. To further substantiate the selectivity, we tested the potencies of these fenamates on two other TRP channels from different subfamilies, TRPC6 and TRPM2. In addition, single-cell Ca^{2+} imaging, whole-cell voltage clamp and insulin secretion experiments revealed mefenamic acid as a selective blocker of TRPM3.

Methods

Cell culture – stable cell lines

Human embryonic kidney (HEK293) cell lines allowing the tetracycline-inducible expression of TRPC6, TRPM2, TRPM3 and TRPV4 were generated using the Flip-In T-Rex-system (Invitrogen, Groningen, the Netherlands) according to the manufacturer's guidelines. Briefly, the cDNAs of TRPC6, TRPM2, TRPM3 and TRPV4 were subcloned in pcDNA5/FRT/TO by amplifying the cDNA fragments and topoisomerase insertion. Flip-In T-Rex 293 cells were grown in Dulbecco's minimum essential medium (DMEM; Biochrom, Berlin, Germany) supplemented with 10% foetal calf serum (Invitrogen), 2 mM L-glutamine (Biochrom), 100 $U \cdot mL^{-1}$ penicillin (Biochrom), 100 $\mu g \cdot mL^{-1}$ streptomycin (Biochrom), 15 $\mu g \cdot mL^{-1}$ blasticidin (Cayla-InvivoGen Europe, Toulouse, France) and 100 $\mu g \cdot mL^{-1}$ zeocin (Cayla-InvivoGen) in the presence of 7% CO_2 atmosphere at 37°C. To generate the cell lines, Flip-In T-Rex 293 cells (100 000 cells 9.6 cm^{-2}) were co-transfected with the pOG44 flipase-coding plasmid DNA and the cDNA-carrying plasmid DNA. Four hours after transfection, the culture medium was replaced by DMEM supplemented with 10% foetal calf serum, 2 mM L-glutamine, 100 $U \cdot mL^{-1}$ penicillin, 100 $\mu g \cdot mL^{-1}$ streptomycin, 15 $\mu g \cdot mL^{-1}$ blasticidin and 75 $\mu g \cdot mL^{-1}$ hygromycin (Cayla-InvivoGen). Several weeks after transfection the growing cells were sorted using the Fluoreporter LacZ Flow Cytometry Kit (Invitrogen) to separate wild-type from recombinant cells. The resulting homogeneous cell population was used for the experiments. The expression of the respective TRP channels were confirmed biochemically by Western blot analyses and/or functionally by Ca^{2+} imaging (Figures S1 and S2).

Fluorescence measurements using FLIPR assay

TRPC6-, TRPM2-, TRPM3- and TRPV4-Flip-In T-Rex 293 cells were seeded in 96-well plates at a density of 8000–12 000 cells per well. One day after seeding, the expression of the recombinant protein was induced by the addition of tetracycline and incubated at 37°C for an additional 18–72 h depending on the cell line. The cells were loaded with 2 μM Fluo-4/AM (Invitrogen) in $CaCl_2$ buffer composed of (mM) 140 NaCl, 5 KCl, 20 HEPES, 2 $CaCl_2$, 2.5 probenecid and 10 glucose for 1 h at 37°C. After loading, cells were washed twice with $CaCl_2$ buffer containing 5 mM $CaCl_2$ and 0.5% dimethyl sulphoxide (DMSO) by an automated plate washer (Denley Cellwash,

Thermo Fisher Scientific Inc., Waltham, MA, USA) and transferred to the FLIPR^{Tetra} (Molecular Devices, Sunnyvale, CA, USA). The FLIPR^{Tetra} integrates a diode array as its excitation source, a 96-well pipettor and a detection system utilizing a CCD imaging camera. Before measurement, 50 µL of the diluted fenamates at a fourfold concentration were simultaneously delivered to all of the wells containing 100 µL. After an incubation period of approximately 10 min, a baseline was recorded and the cells were subsequently stimulated by the simultaneous delivery of 50 µL of the specific activator at a fourfold concentration while fluorescence emissions from the 96 wells were monitored simultaneously at an emission wavelength of 515 nm after excitation with 488 nm (F_{488}). Fluorescence data were collected 60 s before and 4 min after stimulation and analysed off-line.

Amplitudes were transformed to relative fluorescence by normalizing to amplitudes in the absence of fenamates from the same plate, and averaged over 3–4 wells. The fenamates were repeatedly and simultaneously tested under these optimized conditions for their ability to block the TRP channels. The response amplitudes were determined from the fluorescence. Curves were derived from fitting the function

$$f(x) = \frac{a}{1 + e^{-\left(\frac{x - x0}{b}\right)}}$$

to the data by non-linear regression; a = maximum, b = width of transition and $x_0 = IC_{50}$. To establish and compare the rank order of potencies for all compounds, we calculated concentration–response curves from the means of every experiment performed in quadruplicate with regard to a specific TRP channel and substance.

Cell culture – transient expression

HEK293 cells were grown in minimal essential medium (MEM) supplemented with Earl salts (Biochrom), with 10% foetal calf serum (Invitrogen), 2 mM L-glutamine (Biochrom) 100 U·mL^{-1} penicillin (Biochrom) and 100 µg·mL^{-1} streptomycin (Biochrom) in the presence of 5% CO_2 at 37°C. For the experiments, the cells were plated onto glass coverslips placed in 35 mm dishes. For single cell calcium imaging experiments and electrophysiological recordings, the coverslips were coated with poly-L-lysine (Biochrom). One to two days after seeding, the cells were transfected with 2 µg of plasmid DNA coding for TRPM3 C-terminally fused to yellow fluorescent proteins (YFP) using FuGENE HD (Roche Diagnostic, Mannheim, Germany). Two days after transfection, cells were used for experiments.

Single cell fluorescence measurements of HEK293 and INS-1E cells

$[Ca^{2+}]_i$ measurements in single cells were carried out using the fluorescence indicator fura-2-AM in combination with a monochromator-based imaging system (T.I.L.L. Photonics, Gräfeling, Germany) attached to an inverted microscope (Axiovert 100, Carl Zeiss, Oberkochen, Germany). Cells were loaded with 2 µM fura-2-AM (Mobitec, Göttingen, Germany) and 0.01% Pluronic F-127 (Invitrogen) for 30 min at 37°C in a standard solution composed of (in mM) 138 NaCl, 6 KCl, 1 $MgCl_2$, 2 $CaCl_2$, 5.5 glucose or 0.5 glucose/INS-1E cells and 10 HEPES (adjusted to pH 7.4 with NaOH). The osmolarity of the solution which amounts to 300 mosmol·L^{-1} was measured using a freezing point depression osmometer (Roebling, Berlin, Germany). Coverslips were then washed in this buffer for 5 min and mounted in a perfusion chamber on the microscope stage. For $[Ca^{2+}]_i$ measurements, fluorescence was excited at 340 and 380 nm. After correction for background fluorescence, the fluorescence ratio F_{340}/F_{380} was calculated. In all experiments, we identified transfected cells within the whole field of vision by their YFP fluorescence at an excitation wavelength of 480 nm. Experiments with at least 20 cells were summarized and are given as the number of experiments for each experimental condition.

Preparation and single cell fluorescence measurements of islet cells

Islet cells isolated from mice islets by trypsinization as previously described were seeded on glass coverslips in a 35 mm Petri dish and used for experiments after 48–72 h of culture at 37°C (Ullrich *et al.*, 2005). The cells were loaded in culture medium by addition of 2 µM fura-2-AM, 0.02% Pluronic F-127 (Invitrogen) and anion channel blocker sulfinpyrazole (Sigma). The cells were incubated at 37°C for 45 min followed by washing with HBS buffer containing 5 mM glucose and 2.5 mM $CaCl_2$ at 37°C for 15 min. $[Ca^{2+}]_i$ measurements in single cells were carried out using the fluorescence indicator fura-2-AM in combination with a monochromator-based imaging system (T.I.L.L. Photonics, Gräfeling, Germany) attached to an inverted microscope (Axiovert 100, Carl Zeiss, Oberkochen, Germany). For $[Ca^{2+}]_i$ measurements, fluorescence was excited at 340 and 380 nm. After correction for background fluorescence, the fluorescence ratio F_{340}/F_{380} was calculated. Experiments with at least 20 cells were summarized and are given as the number of experiments for each experimental condition.

Patch clamp measurements

Standard whole-cell recordings were performed using an EPC9 amplifier under control of Pulse software (HEKA, Lambrecht, Germany) at room temperature. Pipettes were made from borosilicate glass and had a resistance of 3–5 MΩ. Cells were held at a potential of –15 mV and voltage ramps were performed from –115 to +85 mV (1 mV·ms^{-1}) approximately every second. The pipette solution contained (in mM) 80 CsAsp, 45 CsCl, 10 BAPTA, 10 HEPES, 4 Na_2 ATP or $TRIS_2ATP$, pH was adjusted to 7.2 with CsOH and osmolarity to 305–315 mosmol·L^{-1} with glucose or H_2O. The standard extracellular solution contained (in mM) 145 NaCl, 10 CsCl, 3 KCl, 2 $CaCl_2$, 2 $MgCl_2$, 10 HEPES, 10 D-glucose, pH was adjusted to 7.4 (or as indicated) with NaOH and osmolarity to 315–330 mosmol·L^{-1}. A liquid junction potential of approximately 15 mV, calculated with Clampex (Axon Instruments), was corrected for.

INS-1E cell culture and measurement of insulin secretion

INS-1E cells (a kind gift of Prof Dr C. B. Wollheim, University of Geneva, Switzerland) were cultured in RPMI1640 (Invitrogen) supplemented with (in mM) 10 HEPES, 1 Na^+-pyruvate, 2 glutamine, 0.01 β-mercaptoethanol and 10% (v/v) foetal

calf serum (Invitrogen). For calcium imaging experiments 100 000 cells were seeded onto glass coverslips in a 35 mm petri dish and used for experiments after 48–72 h incubation at 37°C. For insulin secretion experiments, cells were seeded at a density of 1.5×10^5 cells·0.5 mL^{-1} in 24-well plates and incubated as described previously (Ullrich *et al.*, 2005). In brief, after 2 days of culture, cells were preincubated for 30 min in an incubation solution containing (in mM) 140 NaCl, 5.6 KCl, 1.2 $MgCl_2$, 2.6 $CaCl_2$, 10 HEPES, 0.5 glucose and 0.1% bovine serum albumin (BSA fatty acid free, Sigma, Deisenhofen, Germany). Thereafter, cells were incubated for 1 h in the presence of test substances as indicated in a solution without BSA. Insulin released into the supernatant and insulin content after acid ethanol extraction was determined by radioimmunoassay (Linco, USA).

Source of reagents

Flufenamic acid, niflumic acid, mefenamic acid, meclofenamic acid, S645648, tolfenamic acid and pregnenolone sulphate (Sigma-Aldrich, Deisenhofen, Germany) were diluted from 50 mM stock solutions in DMSO. DCDPC (Aventis, Frankfurt, Germany) (Gögelein and Pfannmüller, 1989; Gögelein *et al.*, 1990), and hyperforin (Dr Willmar Schwabe, Karlsruhe, Germany) were used from 50 mM stock solution in DMSO. 4α-Phorbol-12,13-didecanoate was purchased from LC Laboratories (Woburn, MA, USA) and diluted from 10 mM stock solutions. Hydrogen peroxide (Roth, Karlsruhe, Germany) was diluted from the delivered concentrated solution (8.8 M). The anti-TRPC6 antibody was from Millipore (Schwabach, Germany) (Reiser *et al.*, 2005; Huber *et al.*, 2006; Leuner *et al.*, 2007; Müller *et al.*, 2008). The generation and characterization of the antibodies directed against TRPM2, TRPM3 and TRPV4 have been previously described (Grimm *et al.*, 2003; Kraft *et al.*, 2006; Reiter *et al.*, 2006; Hartmannsgruber *et al.*, 2007; Wehrhahn *et al.*, 2010).

Results

Effects of fenamates on TRPM3 and other TRP channels

Flufenamic acid (Figure 1), a fenamate compound, has already been described as blocker of a variety of TRP channels (Tesfai *et al.*, 2001; Lee *et al.*, 2003; Guinamard *et al.*, 2004; Hill *et al.*, 2004; Guilbert *et al.*, 2009). To compare the potency of flufenamic acid with the potencies of other fenamate derivatives (Figure 1) in blocking TRP channel activity, we generated cell lines stably expressing TRP channels from three different subfamilies, TRPC6, TRPM2, TRPM3 and TRPV4, in a tetracycline-regulated manner. Each stable cell line was characterized by Western blotting (Figure S1) and calcium imaging experiments (Figure S2) to test for tetracycline-dependent expression. Hyperforin (10 μM), hydrogen peroxide (5 mM), pregnenolone sulphate (35 μM) and 4α-phorbol-12,13-didecanoate (5 μM) were used as selective activators of TRPC6, TRPM2, TRPM3 and TRPV4 channels, respectively (Hara *et al.*, 2002; Watanabe *et al.*, 2002; Wagner *et al.*, 2008; Leuner *et al.*, 2010). The values of half-maximal inhibition (IC_{50} values) obtained from at least three independent experiments performed in quadruplicate were

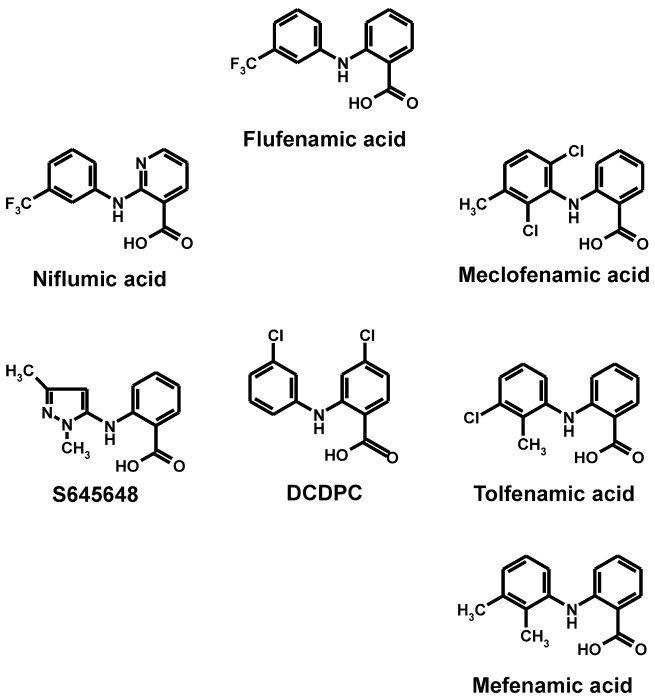

Figure 1

Structures of the fenamates tested. Flufenamic acid (N-[3-(trifluoromethyl)-phenyl]anthranilic acid), niflumic acid (2-{[3-(trifluoromethyl)phenyl]amino}nicotinic acid), S645648 (N-(1,3-dimethyl-5-pyrazolyl) anthranilic acid), DCDPC (3′-5-dichlorodiphenylamine-2-carboxylic acid), meclofenamic acid (N-(2,6-dichloro-3-methylphenyl)anthranilic acid), tolfenamic acid (N-(2-methyl-3-chlorophenyl)anthranilic acid) and mefenamic acid (2-(2,3-dimethylphenyl)aminobenzoic acid).

averaged and are summarized in Table 1A. Several aspects of the obtained IC_{50} values are given as rank-orders of potencies, with respect to the TRP channels (Table 1B) or fenamates analysed (Table 1C). Interestingly, S645648, a dimethyl-pyrazolyl anthranilic acid derivative obtained from the Sigma rare compound collection, failed to block TRP channels and was not considered further. The fenamate niflumic acid, which has been intensively used as a pharmacological tool to interfere with cell volume regulation (Parkerson and Sontheimer, 2003; Moreland *et al.*, 2006; Han *et al.*, 2008), was less potent than flufenamic acid in blocking the four TRP channels in our study. Based on the fact that flufenamic acid has been used for the modulation of TRP channels it was surprising that the mono- and dichloro-methyl-phenyl anthranilic acid derivatives, meclofenamic acid and tolfenamic acid, as well as the mono-chloro-phenyl-chloro anthranilic acid derivative DCDPC, outperformed flufenamic acid in blocking TRP channels, with TRPC6 as the only exception (Table 1A and B). Meclofenamic acid and tolfenamic acid showed the same order of blocking potency for all four TRP channels investigated, whereas DCDPC blocked TRPV4 more potently than TRPC6 (Table 1C). Altogether, and across all four TRP channels tested in our study, DCDPC turned out to be the most potent, non-selective TRP channel blocker with IC_{50} values ranging from 7.5 to 31 μM (Table 1A and B). By contrast, and surprisingly, the selectivity of mefenamic acid for

Table 1

(A) Inhibitory effect (IC_{50} values) of fenamates on transient receptor potential (TRP) channels

	TRPC6	TRPM2	TRPM3	TRPV4
DCDPC	16.4 ± 3.1 μM	31.1 ± 3.4 μM	7.5 ± 4.7 μM	8.6 ± 1.8 μM
Flufenamic acid	17.1 ± 7.2 μM	155.1 ± 50.6 μM	33.1 ± 8.3 μM	40.7 ± 10.3 μM
Niflumic acid	40.2 ± 20.1 μM	>300 μM	123.5 ± 24.3 μM	84.4 ± 11.9 μM
Mefenamic acid	>300 μM	>300 μM	6.6 ± 1.8 μM	>300 μM
Meclofenamic acid	37.5 ± 14.4 μM	75.8 ± 33.6 μM	13.3 ± 3.5 μM	40.7 ± 10.2 μM
S645648	>300 μM	>300 μM	>300 μM	>300 μM
Tolfenamic acid	12.3 ± 4.8 μM	96.1 ± 10.8 μM	11.1 ± 2.7 μM	23.9 ± 7.1 μM

(B) Rank order of fenamates according to their potencies in blocking transient receptor potential (TRP) channels

TRPC6	TOL ~ DCDPC ~ FLU > MEC ~ NIF > S645648, **MEF**
TRPM2	DCDPC > MEC > TOL > FLU > NIF, S645648, **MEF**
TRPM3	**MEF** > DCDPC > TOL ~ MEC > FLU > NIF > S645648
TRPV4	DCDPC > TOL > FLU, MEC > NIF > S645648, **MEF**

(C) Rank order of transient receptor potential (TRP) channels most potently blocked by each fenamate

DCDPC	TRPM3 ~ TRPV4 > TRPC6 > TRPM2
Flufenamic acid	TRPC6 > TRPM3 > TRPV4 > TRPM2
Niflumic acid	TRPC6 > TRPV4 > TRPM3 > TRPM2
Mefenamic acid	TRPM3 >> TRPV4, TRPC6, TRPM2
Meclofenamic acid	TRPM3 > TRPC6 ~ TRPV4 > TRPM2
Tolfenamic acid	TRPM3 ~ TRPC6 > TRPV4 > TRPM2

In (A) changes in $[Ca^{2+}]_i$ were measured using FLIPR^{Tetra} as described in *Methods* (n = 4–6).
Bold type in (B) highlights the selectivity of mefenamic acid in blocking TRPM3.

TRPM3 was outstanding with an IC_{50} of 6.6 μM, which was two orders of magnitude lower than any concentrations that had elicited effects on the other three TRP channels tested (Figure 2A; Table 1A). This exquisite selectivity of mefenamic acid warranted its further characterization in TRPM3-expressing cells.

Characterization of mefenamic acid as a selective TRPM3 blocker

To examine the specific and selective inhibition of TRPM3 activity by mefenamic acid, we performed single-cell calcium imaging experiments. Although during Fluo-4-based FLIPR 96-well imaging experiments the blocker was applied before the application of a specific TRP channel stimuli, in the single-cell calcium imaging experiments we tested whether the order of application affected the blocking activity of mefenamic acid. As shown in Figure 2B, the application of pregnenolone sulphate (35 μM) resulted in a fast and sustained increase in $[Ca^{2+}]_i$ in HEK293 cells that had been transiently transfected with cDNA coding for TRPM3. The subsequent application of mefenamic acid in the presence of an activator, and at maximal active concentrations of 30 μM, quickly and completely reduced the enhanced $[Ca^{2+}]_i$ back to baseline (Figure 2B). These data indicate that the order of application had no impact on the activity of mefenamic acid.

In electrophysiological whole-cell voltage clamp experiments, currents recorded from TRPM3-expressing HEK293 cells showed an instantaneous increase following the application of pregnenolone sulphate (Figure 3A). The currents were blocked by the subsequent application of mefenamic acid. The current–voltage relationships revealed that mefenamic acid completely blocked the inward current, although a small outward current remained (Figure 3B). Mefenamic acid is a weak organic acid with a pKa value of 4.2. Consequently, at physiological pH values, it resides in its ionic form and is unable to cross the lipophilic barrier of the plasma membrane. To determine whether mefenamic acid blocks TRPM3 from inside or outside, we performed whole-cell voltage clamp recordings with mefenamic acid in the pipette solution (Figure 3C and D). In cells perfused with mefenamic acid, pregnenolone sulphate induced outwardly rectifying currents comparable to the experiments performed in the absence of intracellularly perfused mefenamic acid. By contrast, only the extracellular application of mefenamic acid to pregnenolone sulphate-stimulated cells resulted in a fast decline of the inward and outward currents. Although the

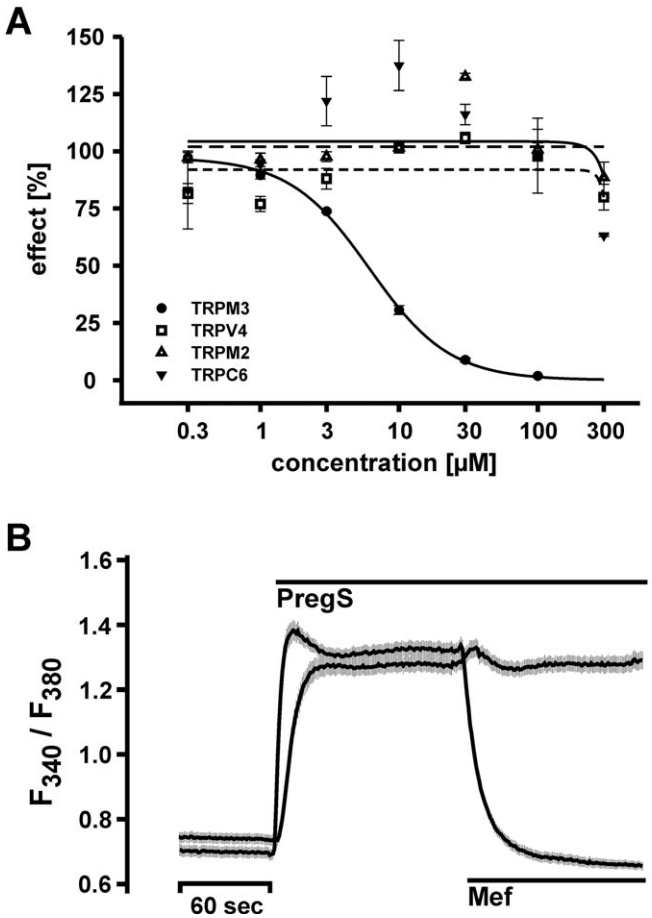

Figure 2

Concentration–response relationship of transient receptor potential (TRP) channel-blocking fenamates. (A) Calcium entry in TRPM3-expressing cells was measured using FLIPR^{Tetra} and data analysed as described in *Methods*. Data from a representative experiment show the effect of mefenamic acid on calcium entry in TRPC6-, TRPM2-, TRPM3- and TRPV4-expressing cells upon hyperforin (10 μM), hydrogen peroxide (5 mM), pregnenolone sulphate (35 μM) and 4α-phorbol-didecanoate (5 μM) stimulation respectively. Mefenamic acid was ineffective at suppressing TRPC6-, TRPM2- and TRPV4-mediated calcium entry, whereas the intracellular calcium concentration ($[Ca^{2+}]_i$) remained at the initial basal level in TRPM3-expressing cells upon stimulation with pregnenolone sulphate. The data were calculated from one experiment of at least three experiments performed in quadruplicate per concentration and TRP channel. (B) In transiently transfected HEK cells expressing TRPM3, the application of pregnenolone sulphate (35 μM) results in an instantaneous increase in intracellular calcium. The application of mefenamic acid (30 μM) during the plateau phase results in a rapid decrease in $[Ca^{2+}]_i$ to basal levels. Application of vehicle had no effect. Mean value obtained from at least 20 cells of one experiment (out of five independent experiments) is shown. The grey shading represents the SEM for each data point.

inward current was almost completely blocked under these conditions, a residual outward current was detectable.

To clarify whether the activity of mefenamic acid, like other organic acids, is pH-dependent, we first analysed whether the pregnenolone sulphate-dependent TRPM3 activity depends on extracellular pH. Pregnenolone sulphate was diluted in solutions with pH adjusted to 8.0, 7.4, 6.6 or 6.0 (Figure S3). The data show that the TRPM3 activity induced by pregnenolone sulphate application is independent of extracellular pH. In a next step, we studied the inhibitory effect of mefenamic acid on pregnenolone sulphate-stimulated inward and outward currents under different extracellular pH conditions in TRPM3-expressing HEK293 cells (Figure 4). At pH 8.0, the amount of residual current during the application of 25 μM mefenamic acid was increased (Figure 4A); at pH 7.4 residual currents were still detectable (Figure 4B), whereas at pH 6.6 and 6.0 any outward or inward currents were completely blocked (Figure 4C). In summary, our experiments clearly show that the activity of mefenamic acid is pH-dependent (Figure 4D and E). Furthermore, Figure 4C shows that the block of TRPM3 by mefenamic acid was reversible because after the washout of mefenamic acid a subsequent application of pregnenolone sulphate induced currents with identical amplitudes, which again could be blocked by mefenamic acid.

Effect of mefenamic acid as a selective TRPM3 blocker in insulin-secreting cells

Based on the characterization of TRPM3 as an ionotropic steroid receptor in pancreatic β-cells and controversial reports on fenamates affecting insulin secretion (Li *et al.*, 2007; Wagner *et al.*, 2008; Fujimoto *et al.*, 2009), we were interested in the effect of mefenamic acid on insulin-secreting pancreatic β-cells. Therefore, we analysed the expression of TRPM3 in insulin-secreting INS-1E cells by Western blot (Figure 5A). Two protein bands were visualized with the anti-TRPM3 antibody (Grimm *et al.*, 2003). The absence of a reaction product when the primary antibody was incubated in the presence of the immunogenic peptide provides evidence of antibody specificity and indicates that the two bands most likely correspond to TRPM3 splice variants with different C-terminal sequences that yield protein of approximately 150 and 220 kDa (Hoffmann *et al.*, 2010). Prior to further functional analysis of INS-1E cells, we tested whether mefenamic acid alters intracellular calcium concentrations in fura-2-loaded INS-1E cells (Figure 5B). As mefenamic acid application had no effect, we next tested whether INS-1E cells functionally express TRPV1, a TRP channel recently described to modulate glucose homeostasis (Razavi *et al.*, 2006). The application of capsaicin in maximal effective concentrations (100 nM) resulted in a fast and large calcium increase, which was insensitive to the application of mefenamic acid (30 μM) (Figure 5C). The application of 35 μM pregnenolone sulphate resulted in an instantaneous and sustained increase in fluorescence ratio indicative of an increase in $[Ca^{2+}]_i$ (Figure 5D). This pregnenolone sulphate-induced Ca^{2+} signal was almost completely counteracted by the application of 30 μM mefenamic acid. By contrast, 30 μM mefenamic acid did not prevent an increase in $[Ca^{2+}]_i$ induced by the application of 20 mM glucose. Thus, the glucose-induced increase in $[Ca^{2+}]_i$ was not affected by mefenamic acid in INS-1E cells (Figure 5D). Blocking ATP-dependent potassium channels with 100 μM tolbutamide, which leads to a depolarization-induced activation of voltage-dependent Ca^{2+} channels, rapidly and strongly increased $[Ca^{2+}]_i$ signals in the presence

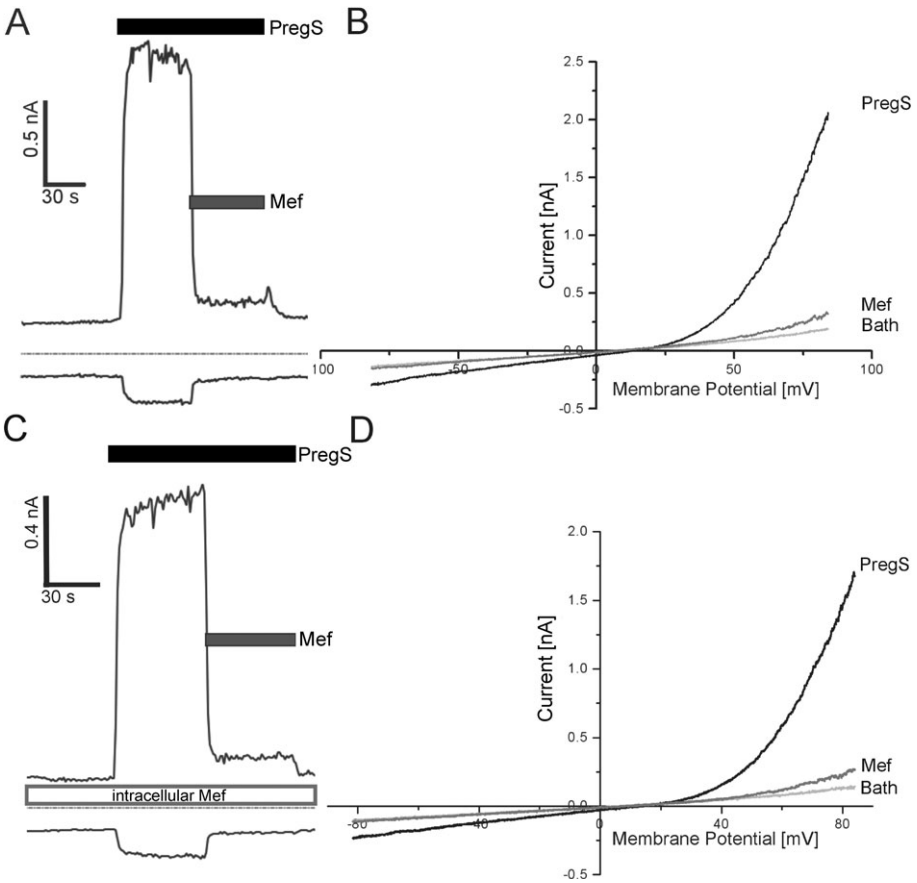

Figure 3

Extracellular application of mefenamic acid inhibits TRPM3 currents in transfected HEK293 cells. (A) Current of TRPM3 at membrane potentials of –80 (lower trace) and +80 mV (upper trace) during the application of the TRPM3 activator pregnenolone sulphate (35 μM) and the inhibition of the current after application of mefenamic acid (25 μM). (B) Current–voltage relationship from experiments shown in (A). Mefenamic acid inhibited the inward current almost completely, although a small outward current is still visible. (C) Current recorded from a TRPM3-expressing cell, experiments performed as in (A) with the modification that mefenamic acid (35 μM) was added into the pipette solution. (D) Current–voltage relationship from the experiment shown in (C). Intracellularly applied mefenamic acid had no impact on the pregnenolone sulphate-induced current.

of mefenamic acid (Figure 5E). The effect of tolbutamide on $[Ca^{2+}]_i$ was further increased by pregnenolone sulphate. The subsequent application of mefenamic acid brought the fluorescence signal back to the level of tolbutamide activation (Figure 5F).

Comparable results were obtained from calcium imaging experiments using fura-2-loaded isolated mouse pancreatic islet cells (Figure 6). Pregnenolone sulphate (Figure 6A) as well as tolbutamide (Figure 6B) induced increases in intracellular calcium concentrations. Whereas the pregnenolone sulphate-induced increases were blocked by mefenamic acid (Figure 6A), the tolbutamide responses were insensitive to fenamate inhibition (Figure 6B). The independence of both calcium entry mechanisms was further supported by the subsequent application of tolbutamide, pregnenolone sulphate and mefenamic acid (Figure 6C). Tolbutamide and subsequent application of pregnenolone sulphate resulted in a two-step increase in intracellular calcium concentrations. Subsequent application of mefenamic acid was able to bring the fluorescence signal back to the level of tolbutamide activation (Figure 6C).

In contrast to the clear impact of TRPM3 activation on calcium entry in insulin-secreting INS-1E cells and mouse islet cells, TRPM3 activation had modulating, synergistic effects on insulin secretion (Wagner *et al.*, 2008). To examine whether the inhibition of the intracellular rise in calcium by mefenamic acid translates into a biological response, we measured the insulin secretion of INS-1E cells (Figure 7). Pregnenolone sulphate, 35 μM, significantly augmented insulin secretion in the presence of tolbutamide, 100 μM, that is, in the presence of closed ATP-dependent potassium channels, as well as in the presence of 12 mM glucose (Figure 7A and B). Mefenamic acid, 30 μM, abolished the stimulation of secretion by pregnenolone sulphate but had not significant effect on tolbutamide-induced insulin secretion and only attenuated glucose-induced secretion. These data suggest that mefenamic acid selectively inhibits the TRPM3-induced modulation of insulin secretion in pancreatic β-cells.

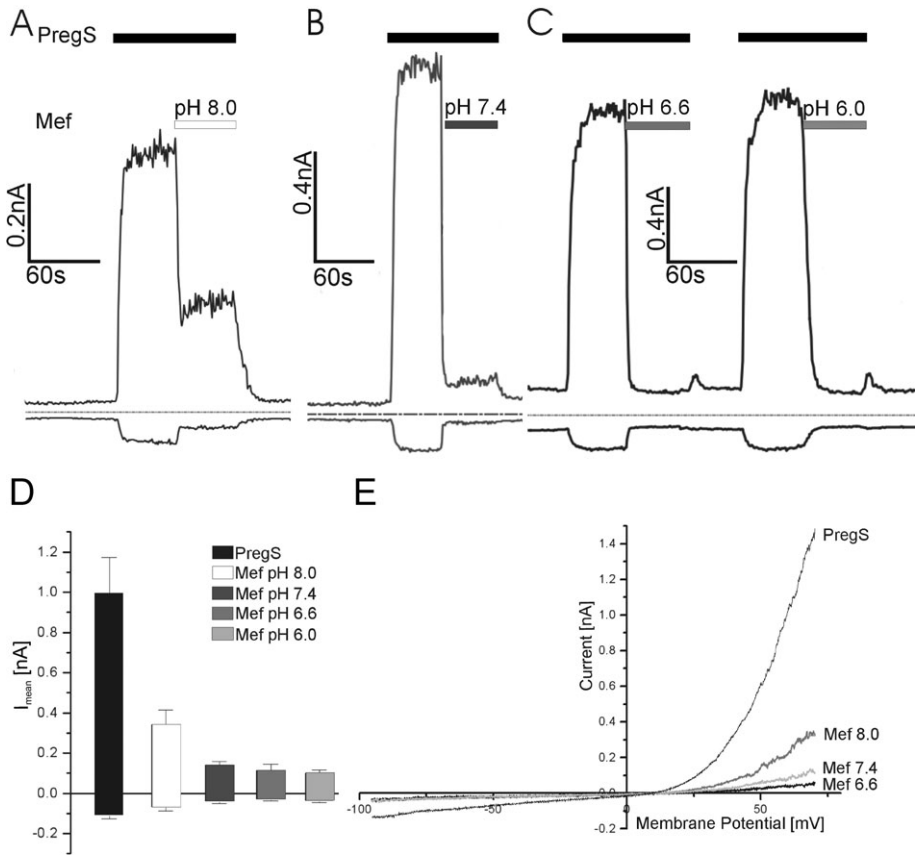

Figure 4

pH-dependence of mefenamic acid on the inhibition of TRPM3-mediated currents. (A) Time course of TRPM3 current at membrane potentials of −80 (lower trace) and +80 mV (upper trace); the pH value of the extracellular solution was 8 before the mefenamic acid (25 μM) was added. (B) Time course of TRPM3 current at membrane potentials of −80 and +80 mV; the pH value of the extracellular solution was 7.4 before the mefenamic acid (25 μM) was added. (C) Time course of TRPM3 current at membrane potentials of −80 and +80 mV; the pH values of the extracellular solution were 6.6 and 6.0 before the mefenamic acid (25 μM) was added. (D) Statistical analysis of experiments performed at pH 8 ($n = 9$), pH 7.4 ($n = 19$), pH 6.6 ($n = 10$) and pH 6 ($n = 9$). (E) Current–voltage relationship from experiments shown in (A–C). Although the inward currents were almost completely inhibited, the block of the outward current was dependent on the pH values.

Discussion

Fenamates are potent inhibitors of cyclooxygenase and therefore used as NSAIDs (Cryer and Feldman, 1998). In addition, fenamates have been studied with respect to their ability and potency to block TRP channels. Within the limitations of our approach, most of this class of compounds can be classified as non-selective TRP channel blockers. Surprisingly, mefenamic acid proved to be a selective blocker of TRPM3.

Fenamates, the N-phenyl-substituted anthranilic acid derivatives, represent an interesting group of small molecules that can be used as pharmacological tools for the characterization and regulation of TRP channels. Since the first description of flufenamic acid as a TRPM2 blocker by Hill *et al.* (2004), the effectiveness of flufenamic acid has been validated by other groups (Tesfai *et al.*, 2001; Lee *et al.*, 2003; Guinamard *et al.*, 2004; Hill *et al.*, 2004; Guilbert *et al.*, 2009). Our results on the potency of flufenamic acid in blocking TRP channels are in line with previous publications regarding the inhibition of TRPM2 and TRPC6 activity by flufenamic acid. Beyond blocking TRPM2 and TRPC6 channels, we now show that flufenamic acid also blocks TRPM3 and TRPV4 channels. The data show that flufenamic acid as well as other fenamate derivatives can be classified as broad range TRP channel blockers, because the compounds block at least four different TRP channels from three different subfamilies and with quite different pore structures. Next to N-(p-amylcinnamoyl) anthranilic acid (ACA), a compound with a phenylcinnamoyl structure, fenamates represent a second class of broad range TRP channel blockers (Kraft *et al.*, 2006; Harteneck *et al.*, 2007). Whereas flufenamic acid is less potent than ACA in blocking TRP channels, other fenamate derivatives such as tolfenamic acid or DCDPC now seem to have potencies comparable with ACA. Thus, tolfenamic acid or DCDPC are much more suitable tools than flufenamic acid. Roughly, our data suggest that the newly tested compounds tolfenamic acid or DCDPC are at least 10-fold more potent than flufenamic acid.

The results presented here demonstrate that mefenamic acid blocks TRPM3 from the outside and that the potency of its inhibitory action depends on the extracellular pH. Hill

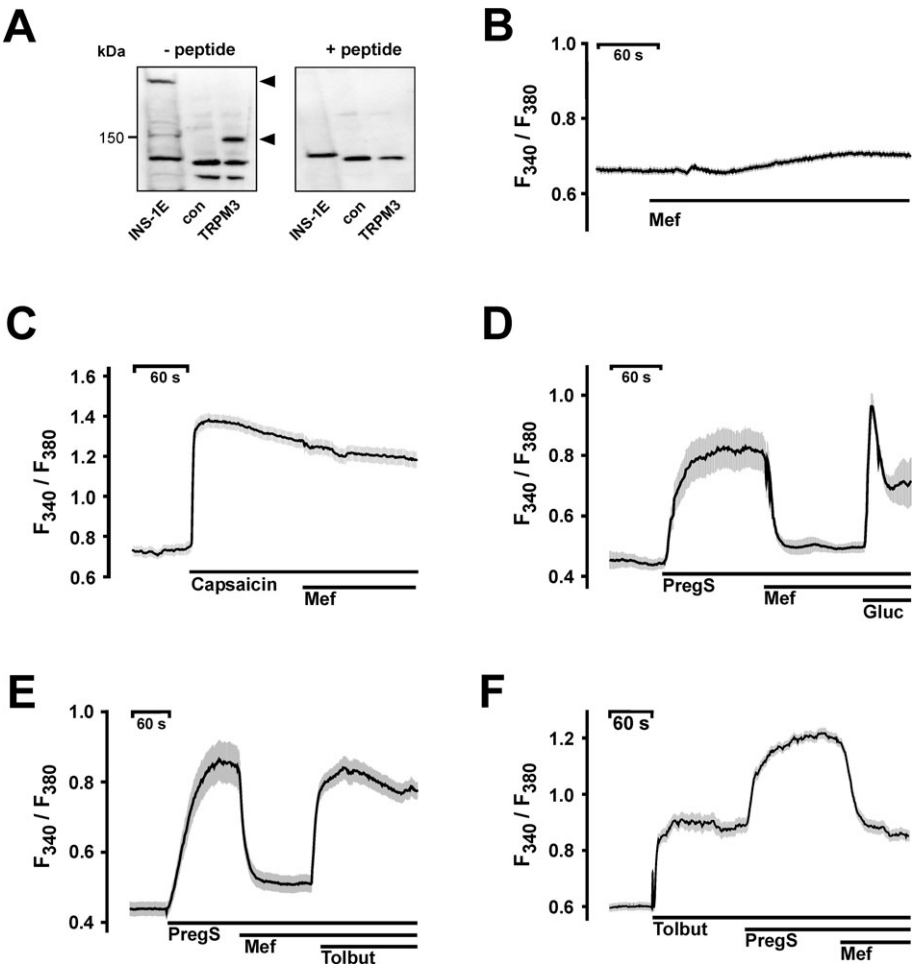

Figure 5

Effects of mefenamic acid on pancreatic β-cells. A. Western blot analysis of membranes extracted from INS-1E cells, HEK293 control cells (con) and TRPM3-expressing HEK293 cells (TRPM3). The anti-TRPM3 antibody detected two bands of approx. 150 and 220 kDa (left panel, – peptide). In the presence of the immunogenic peptide the TRPM3-specific signals were absent (right panel, +peptide). B–F. Changes in $[Ca^{2+}]_i$ are depicted by the fluorescence ratios F_{340}/F_{380} of Fura-2-loaded INS-1E cells. B. Application of mefenamic acid (Mef) did not alter intracellular calcium concentrations. C. Application of capsaicin (100 nM) resulted in a pronounced increase in calcium which was unaffected by mefenamic acid. D. Measurement of $[Ca^{2+}]_i$ of INS-1E cells after stimulation with 35 μM pregnenolone sulphate and block with 30 μM mefenamic acid. An additional stimulus with 20 mM glucose (Gluc) in the presence of 35 μM pregnenolone sulphate and 30 μM mefenamic acid triggered a second increase in $[Ca^{2+}]_i$. E. Mefenamic acid had no effect on voltage-gated calcium channels activated by 100 μM tolbutamide (Tolbut) after blocking pregnenolone sulphate (35 μM)-stimulated INS-1E cells. F. Tolbutamide (100 μM) increased the $[Ca^{2+}]_i$ of INS-1E cells. The application of 35 μM pregnenolone sulphate further enhanced $[Ca^{2+}]_i$, an effect reversed by mefenamic acid. The black lines indicate mean values from at least four independent experiments with at least 20 cells each. The shaded areas depict the SEM for each data point.

et al. (2004) described comparable features for the TRPM2–flufenamic acid interaction, however with important differences. Whereas in the case of TRPM2 additional factors like TRPM2 activation as well as time period of inhibitor application modulate the recovery rate, TRPM3 currents recover instantaneously after washout. Given that flufenamic acid represents a blocker of a broad range of TRP channels together with the fact that both fenamates act from the outside, they might represent channel pore inhibitors. This conclusion is further supported by the fact that the channel proteins of the classic-, melastatin- and vanilloid-like TRP families have a highly conserved pore structure. By contrast, the sequences within the second and/or third transmembrane domains, being generally accepted as binding domains for the activating ligands, dramatically differ in their primary protein sequences (Jordt and Julius, 2002).

Pancreatic β-cells express a variety of ion channels including TRPM3 as shown here and a variety of other TRP channel proteins. Members of the TRPC channel have been described in the context of the modulation of membrane potential via calcium oscillations (Sakura and Ashcroft, 1997; Roe *et al*., 1998; Qian *et al*., 2002): TRPM5, a modulator of receptor-induced calcium signalling (Prawitt *et al*., 2003), TRPM2, a lysosomal intracellular cation channel or a temperature-regulated redox sensor (Togashi *et al*., 2006; Bari *et al*., 2009; Lange *et al*., 2009) and TRPV4, a mechanosensitive cation channel stimulated by human islet amyloid polypeptide (Casas *et al*., 2008). Our study now provides strong evidence

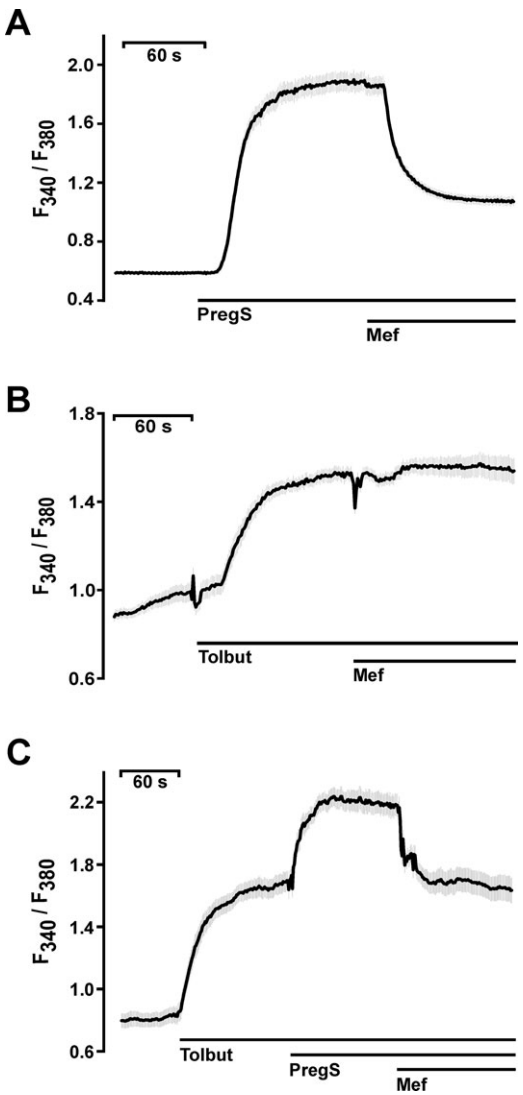

Figure 6

Effects of mefenamic acid on primary mouse pancreatic β-cells. Changes in $[Ca^{2+}]_i$ are depicted by the fluorescence ratios F_{340}/F_{380} of Fura-2-loaded primary mouse pancreatic islet cells. (A) Measurement of $[Ca^{2+}]_i$ after stimulation with 35 μM pregnenolone sulphate and block with 30 μM mefenamic acid. (B) Mefenamic acid (30 μM) had no effect on $[Ca^{2+}]_i$ increased by 100 μM tolbutamide (Tolbut). (C) Tolbutamide (100 μM) increased the $[Ca^{2+}]_i$ in mouse β-cells. The addition of 35 μM pregnenolone sulphate further enhanced $[Ca^{2+}]_i$, an effect reversed by the application of mefenamic acid. The black lines indicate mean values from at least four independent experiments with at least 20 cells each. The shaded areas depict the SEM for each data point.

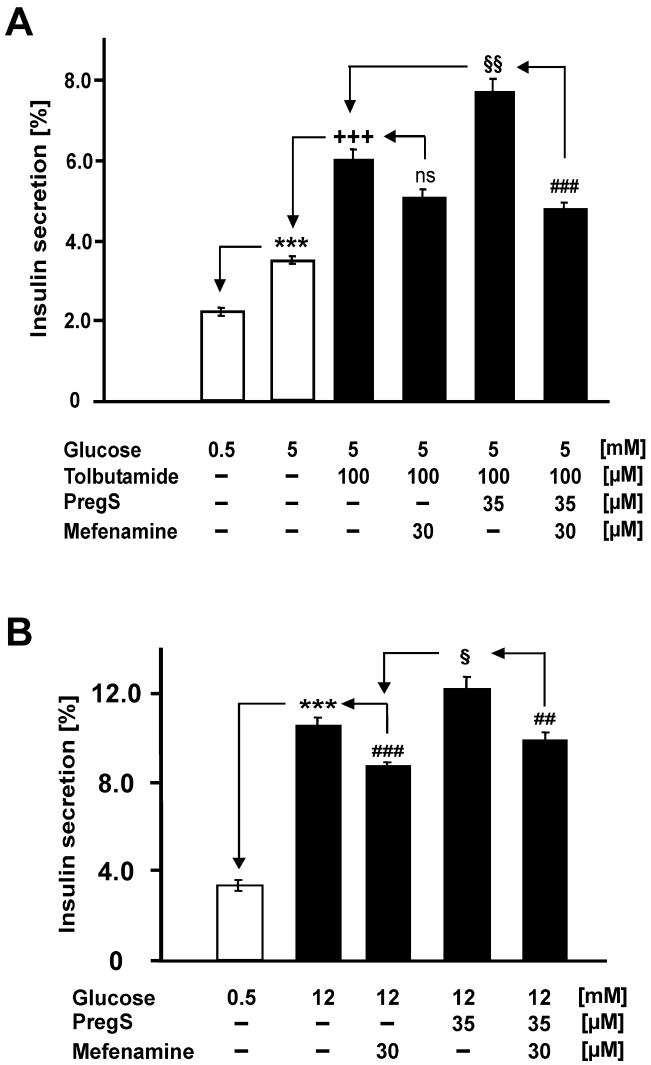

Figure 7

Pregnenolone sulphate-mediated insulin secretion is inhibited by mefenamic acid. INS-1E cells were cultured and insulin secretion measured as described in *Methods*. Test substances were added as indicated. (A) The effect of pregnenolone sulphate and mefenamic acid in the presence of 100 μM tolbutamide. (B) The effect of pregnenolone sulphate and mefenamic acid on insulin secretion induced by 12 mM glucose. Data are means ± SEM of three independent experiments. ***$P < 0.001$ to 0.5 mM glucose; +++$P < 0.001$ to 5 mM glucose; ##$P < 0.005$ and ###$P < 0.001$ to the respective condition without mefenamic acid; §$P < 0.05$ and §§$P < 0.005$ to the respective condition without pregnenolone sulphate; ns, not significant.

that the specific stimulation of TRPM3 augments cytosolic Ca^{2+} and increases insulin secretion, whereas the specific inhibition of TRPM3 by mefenamic acid has almost no effect on glucose-induced insulin secretion. Therefore, the identification of mefenamic acid as a TRPM3 channel inhibitor is remarkable not only as a pharmacological tool but also from another point of view. Mefenamic acid, assigned as an NSAID, is clinically used in many countries to treat pain of moderate severity, dysmenorrhoea, headache and dental pain. In conventional pharmacological textbooks, the analgesic effect of fenamates is explained by cyclooxygenase inhibition interfering with the production of the local hormones of the arachidonic pathway. A link to glucose metabolisms or diabetes cannot be found; nevertheless, it exists when consulting other resources, for example the database of the American Hospital Formulary Service or the available package leaflets of mefenamic acid formulations. The recommendation to control blood glucose levels in diabetic patients also provides

indirect evidence for the clinical relevance of our findings and physiological relevance for TRPM3 in blood glucose homeostasis. This recommendation is a mefenamic acid-specific feature because mefenamic acid is used clinically in daily doses of 500 to 1000 mg, resulting in a mean serum concentration of around 82.9 μM (Cryer and Feldman, 1998). With 90% protein binding of mefenamic acid, the resulting 8.3 μM free serum concentration is in the range of the half-maximal inhibition of TRPM3 (IC_{50} 8.6 μM). Despite this evidence, the physiological role and underlying TRPM3-dependent signalling pathway has to be analysed.

In summary, we have shown that fenamates represent a group of interesting drugs for the modulation of TRP channel function. Although most of the structures tested blocked TRP channels in a non-selective manner, mefenamic acid was identified and characterized as a selective TRPM3 blocking agent. This TRPM3 selectivity was shown in heterologous expression systems as well as in insulin-secreting cells endogenously expressing TRPM3. Mefenamic acid selectively blocked TRPM3-mediated calcium entry and insulin secretion. A combination of molecular and clinical analyses of mefenamic acid will provide further insights into the physiological role of TRPM3 with the prospect of a new molecular approach to interfere with diabetes.

Acknowledgements

The authors thank Sieglinde Haug for technical help. The authors were supported by grants from the Deutsche Forschungsgemeinschaft (HA2800/1-3, HA2800/4-1 and UL140/7-1) and a grant of the German Federal Ministry of Education and Research (BMBF) to the German Center of Diabetes Research (DzD e. V.).

Conflict of interest

The authors state no conflict of interest.

References

Bari MR, Akbar S, Eweida M, Kühn FJ, Gustafsson AJ, Lückhoff A *et al.* (2009). H_2O_2-induced Ca^{2+} influx and its inhibition by N-(p-amylcinnamoyl)anthranilic acid in the beta-cells: involvement of TRPM2 channels. J Cell Mol Med 13: 3260–3267.

Beech DJ, Bahnasi YM, Dedman AM, Al-Shawaf E (2009). TRPC channel lipid specificity and mechanisms of lipid regulation. Cell Calcium 45: 583–588.

Casas S, Novials A, Reimann F, Gomis R, Gribble FM (2008). Calcium elevation in mouse pancreatic beta cells evoked by extracellular human islet amyloid polypeptide involves activation of the mechanosensitive ion channel TRPV4. Diabetologia 51: 2252–2262.

Caspani O, Heppenstall PA (2009). TRPA1 and cold transduction: an unresolved issue? J Gen Physiol 133: 245–249.

Clapham DE, Julius D, Montell C, Schultz G (2005). International Union of Pharmacology. XLIX. Nomenclature and structure-function relationships of transient receptor potential channels. Pharmacol Rev 57: 427–450.

Cryer B, Feldman M (1998). Cyclooxygenase-1 and cyclooxygenase-2 selectivity of widely used nonsteroidal anti-inflammatory drugs. Am J Med 104: 413–421.

Delmas P (2005). Polycystins: polymodal receptor/ion-channel cellular sensors. Pflügers Arch 451: 264–276.

Ducharme G, Newell EW, Pinto C, Schlichter LC (2007). Small-conductance Cl^- channels contribute to volume regulation and phagocytosis in microglia. Eur J Neurosci 26: 2119–2130.

Dvorzhak AY (2008). Effects of fenamate on inhibitory postsynaptic currents in Purkinje's cells. Bull Exp Biol Med 145: 564–568.

Fujimoto W, Miki T, Ogura T, Zhang M, Seino Y, Satin LS *et al.* (2009). Niflumic acid-sensitive ion channels play an important role in the induction of glucose-stimulated insulin secretion by cyclic AMP in mice. Diabetologia 52: 863–872.

Gögelein H, Pfannmüller B (1989). The nonselective cation channel in the basolateral membrane of rat exocrine pancreas. Inhibition by 3',5-dichlorodiphenylamine-2-carboxylic acid (DCDPC) and activation by stilbene disulfonates. Pflügers Arch 413: 287–298.

Gögelein H, Dahlem D, Englert HC, Lang HJ (1990). Flufenamic acid, mefenamic acid and niflumic acid inhibit single nonselective cation channels in the rat exocrine pancreas. FEBS Lett 268: 79–82.

Grimm C, Kraft R, Sauerbruch S, Schultz G, Harteneck C (2003). Molecular and functional characterization of the melastatin-related cation channel TRPM3. J Biol Chem 278: 21493–21501.

Guilbert A, Gautier M, Dhennin-Duthille I, Haren N, Sevestre H, Ouadid-Ahidouch H (2009). Evidence that TRPM7 is required for breast cancer cell proliferation. Am J Physiol Cell Physiol 297: C493–C502.

Guinamard R, Chatelier A, Demion M, Potreau D, Patri S, Rahmati M *et al.* (2004). Functional characterization of a Ca^{2+}-activated non-selective cation channel in human atrial cardiomyocytes. J Physiol 558: 75–83.

Habjan S, Vandenberg RJ (2009). Modulation of glutamate and glycine transporters by niflumic, flufenamic and mefenamic acids. Neurochem Res 34: 1738–1747.

Han JH, Bai GY, Park JH, Yuan K, Park WH, Kim SZ *et al.* (2008). Regulation of stretch-activated ANP secretion by chloride channels. Peptides 29: 613–621.

Hara Y, Wakamori M, Ishii M, Maeno E, Nishida M, Yoshida T *et al.* (2002). LTRPC2 Ca^{2+}-permeable channel activated by changes in redox status confers susceptibility to cell death. Mol Cell 9: 163–173.

Harteneck C (2005). Function and pharmacology of TRPM cation channels. Naunyn Schmiedebergs Arch Pharmacol 371: 307–314.

Harteneck C, Plant TD, Schultz G (2000). From worm to man: three subfamilies of TRP channels. Trends Neurosci 23: 159–166.

Harteneck C, Frenzel H, Kraft R (2007). N-(p-amylcinnamoyl)anthranilic acid (ACA): a phospholipase A_2 inhibitor and TRP channel blocker. Cardiovasc Drug Rev 25: 61–75.

Hartmannsgruber V, Heyken WT, Kacik M, Kaistha A, Grgic I, Harteneck C *et al.* (2007). Arterial response to shear stress critically depends on endothelial TRPV4 expression. PLoS ONE 2: e827.

Hill K, Benham CD, McNulty S, Randall AD (2004). Flufenamic acid is a pH-dependent antagonist of TRPM2 channels. Neuropharmacology 47: 450–460.

Hoffmann A, Grimm C, Kraft R, Goldbaum O, Wrede A, Nolte C *et al.* (2010). TRPM3 is expressed in sphingosine-responsive myelinating oligodendrocytes. J Neurochem 114: 654–665.

Huber TB, Schermer B, Müller RU, Höhne M, Bartram M, Calixto A *et al.* (2006). Podocin and MEC-2 bind cholesterol to regulate the activity of associated ion channels. Proc Natl Acad Sci USA 103: 17079–17086.

Jin NG, Kim JK, Yang DK, Cho SJ, Kim JM, Koh EJ *et al.* (2003). Fundamental role of ClC-3 in volume-sensitive Cl^- channel function and cell volume regulation in AGS cells. Am J Physiol Gastrointest Liver Physiol 285: G938–G948.

Jordt SE, Julius D (2002). Molecular basis for species-specific sensitivity to 'hot' chili peppers. Cell 108: 421–430.

Kankaanranta H, Moilanen E (1995). Flufenamic and tolfenamic acids inhibit calcium influx in human polymorphonuclear leukocytes. Mol Pharmacol 47: 1006–1013.

Kraft R, Harteneck C (2005). The mammalian melastatin-related transient receptor potential cation channels: an overview. Pflügers Arch 451: 204–211.

Kraft R, Grimm C, Frenzel H, Harteneck C (2006). Inhibition of TRPM2 cation channels by N-(p-amylcinnamoyl)anthranilic acid. Br J Pharmacol 148: 264–273.

Lambert S, Oberwinkler J (2005). Characterization of a proton-activated, outwardly rectifying anion channel. J Physiol 567: 191–213.

Lange I, Yamamoto S, Partida-Sanchez S, Mori Y, Fleig A, Penner R (2009). TRPM2 functions as a lysosomal Ca^{2+}-release channel in beta cells. Sci Signal 2: ra23.

Lee YM, Kim BJ, Kim HJ, Yang DK, Zhu MH, Lee KP *et al.* (2003). TRPC5 as a candidate for the nonselective cation channel activated by muscarinic stimulation in murine stomach. Am J Physiol Gastrointest Liver Physiol 284: G604–G616.

Leuner K, Kazanski V, Müller M, Essin K, Henke B, Gollasch M *et al.* (2007). Hyperforin – a key constituent of St. John's wort specifically activates TRPC6 channels. FASEB J 21: 4101–4111.

Leuner K, Heiser JH, Derksen S, Mladenov MI, Fehske CJ, Schubert R *et al.* (2010). Simple 2,4 diacylphloroglucinols as TRPC6 activators – identification of a novel pharmacophore. Mol Pharmacol 77: 368–377.

Li J, Zhang N, Ye B, Ju W, Orser B, Fox JE *et al.* (2007). Non-steroidal anti-inflammatory drugs increase insulin release from beta cells by inhibiting ATP-sensitive potassium channels. Br J Pharmacol 151: 483–493.

Montell C, Rubin GM (1989). Molecular characterization of the Drosophila trp locus: a putative integral membrane protein required for phototransduction. Neuron 2: 1313–1323.

Montell C, Birnbaumer L, Flockerzi V, Bindels RJ, Bruford EA, Caterina MJ *et al.* (2002). A unified nomenclature for the superfamily of TRP cation channels. Mol Cell 9: 229–231.

Moreland JG, Davis AP, Bailey G, Nauseef WM, Lamb FS (2006). Anion channels, including ClC-3, are required for normal neutrophil oxidative function, phagocytosis, and transendothelial migration. J Biol Chem 281: 12277–12288.

Müller M, Essin K, Hill K, Beschmann H, Rubant S, Schempp CM *et al.* (2008). Specific TRPC6 channel activation, a novel approach to stimulate keratinocyte differentiation. J Biol Chem 283: 33942–33954.

Numata T, Wehner F, Okada Y (2007). A novel inhibitor of hypertonicity-induced cation channels in HeLa cells. J Physiol Sci 57: 249–252.

Parkerson KA, Sontheimer H (2003). Contribution of chloride channels to volume regulation of cortical astrocytes. Am J Physiol Cell Physiol 284: C1460–C1467.

Prawitt D, Monteilh-Zoller MK, Brixel L, Spangenberg C, Zabel B, Fleig A *et al.* (2003). TRPM5 is a transient Ca^{2+}-activated cation channel responding to rapid changes in $[Ca^{2+}]_i$. Proc Natl Acad Sci USA 100: 15166–15171.

Puertollano R, Kiselyov K (2009). TRPMLs: in sickness and in health. Am J Physiol Renal Physiol 296: F1245–F1254.

Qian F, Huang P, Ma L, Kuznetsov A, Tamarina N, Philipson LH (2002). TRP genes: candidates for nonselective cation channels and store-operated channels in insulin-secreting cells. Diabetes 51 (Suppl. 1): S183–S189.

Razavi R, Chan Y, Afifiyan FN, Liu XJ, Wan X, Yantha J *et al.* (2006). $TRPV1^+$ sensory neurons control β cell stress and islet inflammation in autoimmune diabetes. Cell 127: 1123–1135.

Reiser J, Polu KR, Moller CC, Kenlan P, Altintas MM, Wei C *et al.* (2005). TRPC6 is a glomerular slit diaphragm-associated channel required for normal renal function. Nat Genet 37: 739–744.

Reiter B, Kraft R, Günzel D, Zeissig S, Schulzke JD, Fromm M *et al.* (2006). TRPV4-mediated regulation of epithelial permeability. FASEB J 20: 1802–1812.

Roe MW, Worley JF, 3rd, Qian F, Tamarina N, Mittal AA, Dralyuk F *et al.* (1998). Characterization of a Ca^{2+} release-activated nonselective cation current regulating membrane potential and $[Ca^{2+}]_i$ oscillations in transgenically derived beta-cells. J Biol Chem 273: 10402–10410.

Sakura H, Ashcroft FM (1997). Identification of four trp1 gene variants murine pancreatic beta-cells. Diabetologia 40: 528–532.

Talavera K, Nilius B, Voets T (2008). Neuronal TRP channels: thermometers, pathfinders and life-savers. Trends Neurosci 31: 287–295.

Tesfai Y, Brereton HM, Barritt GJ (2001). A diacylglycerol-activated Ca^{2+} channel in PC12 cells (an adrenal chromaffin cell line) correlates with expression of the TRP-6 (transient receptor potential) protein. Biochem J 358: 717–726.

Togashi K, Hara Y, Tominaga T, Higashi T, Konishi Y, Mori Y *et al.* (2006). TRPM2 activation by cyclic ADP-ribose at body temperature is involved in insulin secretion. EMBO J 25: 1804–1815.

Ullrich S, Berchtold S, Ranta F, Seebohm G, Henke G, Lupescu A *et al.* (2005). Serum- and glucocorticoid-inducible kinase 1 (SGK1) mediates glucocorticoid-induced inhibition of insulin secretion. Diabetes 54: 1090–1099.

Vennekens R, Owsianik G, Nilius B (2008). Vanilloid transient receptor potential cation channels: an overview. Curr Pharm Des 14: 18–31.

Vietri M, De Santi C, Pietrabissa A, Mosca F, Pacifici GM (2000). Fenamates and the potent inhibition of human liver phenol sulphotransferase. Xenobiotica 30: 111–116.

Vriens J, Appendino G, Nilius B (2009). Pharmacology of vanilloid transient receptor potential cation channels. Mol Pharmacol 75: 1262–1279.

Wagner TF, Loch S, Lambert S, Straub I, Mannebach S, Mathar I *et al.* (2008). Transient receptor potential M3 channels are ionotropic steroid receptors in pancreatic beta cells. Nat Cell Biol 10: 1421–1430.

Watanabe H, Davis JB, Smart D, Jerman JC, Smith GD, Hayes P *et al.* (2002). Activation of TRPV4 channels (hVRL-2/mTRP12) by phorbol derivatives. J Biol Chem 277: 13569–13577.

Wehrhahn J, Kraft R, Harteneck C, Hauschildt S (2010). Transient receptor potential melastatin 2 is required for lipopolysaccharide-induced cytokine production in human monocytes. J Immunol 184: 2386–2393.

Supporting information

Additional Supporting Information may be found in the online version of this article:

Figure S1 Biochemical characterization of the stably transient receptor potential (TRP) channel-expressing cell lines. For the Western blot analysis of the tetracycline-inducible expression of TRP channels, membrane proteins extracted from cell line stably expressing of TRPC6 (A), TRPM2 (B), TRPM3 (C) and TRPV4 (D) grown in the absence or presence of tetracycline (2.5 mg·mL^{-1}) were separated by SDS-PAGE electrophoresis and transferred onto nitrocellulose membranes as previously described by Kraft *et al.* (2006). Immobilized proteins were visualized by using specific antibodies. The anti-TRPC6 antibody was from Millipore (Schwabach, Germany). The generation and characterization of the antibodies directed against TRPM2, TRPM3 and TRPV4 have been previously described (Grimm *et al.*, 2003; Kraft *et al.*, 2006; Reiter *et al.*, 2006). The anti-TRPV4 antibody visualized two bands, the glycosylated and unglycosylated TRPV4 protein, described by Xu *et al* (2006).

Figure S2 Functional characterization of the stable transient receptor potential (TRP) channel-expressing cell lines. Cells stably expressing the TRP channel in a tetracycline-dependent manner were seeded and expression was induced by the addition of tetracycline (2.5 mg·mL^{-1}). For calcium imaging, cells were loaded with Fluo-4. Fluo-4-dependent fluorescence was recorded in the presence or absence of the specific stimulus (arrow). (A) TRPC6-expressing cells were stimulated with hyperforin (10 μM). (B) TRPM2-expressing cells were stimulated with hydrogen peroxide (H2O2; 5 mM). (C) TRPM3-expressing cells were stimulated with pregnenolone sulphate (PregS; 35 μM). (D) TRPV4-expressing cells were stimulated with 4α-phorbol-didecanoate (PDD; 5 μM). Shown are representative traces recorded from 10 000 cells. Subsequently to the initial validation of functional expression, optimal time periods in the presence of tetracycline were determined. The optimal expression levels of TRPC6, TRPM2, TRPM3 and TRPV4 were achieved 72, 24, 72 and 20 h after expression induction by tetracycline respectively (data not shown). The incubation time have been determined experimentally and represent a compromise between optimal signal resulting from expression level and signal-to-noise ratio determined by the loss of cells during loading and washing procedures due to increased intracellular calcium concentration in TRP channel-expressing cells leading to rounding and displacing of the cells.

Figure S3 Activation of TRPM3 by pregnenolone sulphate is independent of pH. (A) Currents of TRPM3 at membrane potentials of –80 (upper trace) and +80 mV (lower trace) recorded during extracellular application of the TRPM3 activator pregnenolone sulphate (35 μM) diluted in extracellular solutions with pH adjusted to 7.4 or 6.0 as indicated. (B) Currents obtained under comparable experimental conditions as used in (A), however the pH of the extracellular solutions was adjusted to pH 7.4, 8.0 or 6.6 as indicated. (C,D) Current-voltage relationship from experiments shown in (A,B), respectively, show that the pregnenolone sulphate-dependent stimulation of TRPM3 is independent of extracellular pH. (E) Statistical analysis of experiments performed at pH 7.4 (n = 5), pH 6.0 (n = 7), pH 6.6 (n = 6) and pH 8.0 (n = 6).

Please note: Wiley-Blackwell are not responsible for the content or functionality of any supporting materials supplied by the authors. Any queries (other than missing material) should be directed to the corresponding author for the article.